Energy dependence of angular distributions of sputtered particles from the Ag{111} surface

Che-Chen Chang
Department of Chemistry, University of Hawaii, Honolulu, Hawaii 96822
and Department of Chemistry, National Taiwan University, Taipei, Taiwan, Republic of China
(Received 16 February 1993)

The angular distributions of Ag atoms ejected from a Ag{111} surface due to 2-keV Ar bombardment have been calculated from molecular-dynamics simulations of the particle impact event. For atoms ejected with kinetic energies of above 15 eV, the distributions are found to be sensitive to variations in the ejection energy. The direction along which the maximum sputter intensity is detected alternates between two different ⟨211⟩ azimuths as the kinetic energy of the ejected atom is increased. A time-exposure representation of the surface-collision cascade is introduced for examining the collision mechanisms that cause atoms to eject along specific crystallographic directions. It shows that, in addition to the presence of the open spacings between the first-layer surface atoms, there are subtle collision effects that determine the preferred direction of ejection. Atomic ejection along those ⟨211⟩ azimuths which have the non-close-packed row of atoms extending to the bulk is mainly induced by the up-down-, the head-on-, and the sideswipe-collision processes. The up-down-collision process may result in ejection of atoms at a distance of more than 20 Å away from the point of the primary impact. Further, the low-energy atoms are usually emitted from the surface due to sideswipe collisions by the moving surface atoms. The dependence of the preferred direction of ejection on the collision time of the ejected atom is also discussed.

I. INTRODUCTION

The measurement of the angular distributions of sputtered particles has been a useful approach to characterize solid surfaces.[1–4] Rather than collect sputtered particles over all angles and energies, one may selectively detect, as a function of their takeoff angle, those particles at specific ejection energies so that structure sensitive information about the surface may be obtained. The resulting angular distribution is found to be determined by the presence of open spacings in the top surface layer.[5] Atoms around these spacings may provide strong directional forces on ejecting particles and render preferential ejection of the particles along specific crystallographic directions. This is particularly true for particles ejecting from a close-packed surface such as the {111} face of the face-centered-cubic crystal structure.[5] Determination of the surface structure by measuring the angular distribution of the particles sputtered from the surface forms the basis for surface characterization using the techniques of angle-resolved mass spectrometry.[6–9]

In the past, the angle-resolved mass spectrometric measurement has been performed with a pass energy of less than 50 eV and with a bandwidth of as small as 2 eV.[1–3,7–12] Questions arise as to the angular distribution of sputtered particles at any specific ejection energy. Results from the theoretical modeling of the collision process in the surface have shown that particles emitted at lower kinetic energies tend to eject late in the collision cascade, i.e., at the time when the surface is much disturbed by the incident beam.[5] The higher energy particles, on the other hand, tend to eject early in the trajectory when the surface order is still present.[5,7,13] The resulting angular distribution of the high-energy particles is thus well defined, due to the channeling of the particles through open spacings in the top surface layer, and better reflects the structure of the sample surface than that of the low-energy particles. Accordingly, one would expect that the sputtered particles of any high ejection energies may be collected for precisely determining the geometric structure of the surface. It implies that the azimuthal direction at which the maximum sputter intensity is observed does not change with the ejection energy.

In this study, the determination of surface structures at any high energies of ejection is investigated. Specifically, molecular-dynamics calculations are performed (i) to examine the sensitivity of the angular distribution to variations of the ejection energy in the high kinetic-energy regime of above 5 eV, and (ii) to understand the type of mechanism through which atoms are ejected along particular crystallographic directions. We find that, as predicted by the theory, the angular distribution of ejected particles does not change significantly with the kinetic energy of ejection when the energy is less than 15 eV. These particles are preferentially ejected along the ⟨211⟩ azimuths which have close-packed rows of atoms extending to the bulk. However, as the kinetic energy of ejection is increased to more than 15 eV, the preferred direction of ejection alternates between two different ⟨211⟩ azimuths, one along the close-packed ⟨211⟩ direction and the other along the non-close-packed direction. In order to better understand the variation of the angular distribution with the ejection energy, we introduce a time-exposure representation of the collision cascade in the surface. This representation allows us to explore, in the atomic level, the collision mechanisms that cause particles to take off from the surface with specific directions and energies. Collision mechanisms which result in the

alternation of the azimuth of the maximum sputter intensity are found to be related to both the surface atomic arrangement along the direction of ejection and the details of the atomic scattering process in the surface. Atoms which eject along the non-close-packed ⟨211⟩ azimuth may result from either the up-down-, the head-on-, or the sideswipe-collision processes with the moving neighboring atoms originally positioned as far as more than 5 Å away from the ejecting atoms. Finally, the dependence of the angular distribution of ejected atoms on the collision time is explored. Our results show that the angular distribution may also be affected by the time interval between the instant of the primary impact on the surface and the moment when the emitting atom is out of the interaction range with the surface.

II. CALCULATIONAL METHOD

The dynamics of the surface-collision process which is initiated by the energetic incident particle is modeled using the computation scheme previously developed by Harrison and co-workers.[14] In this study, Ar atoms of 2-keV kinetic energy are allowed to impinge at normal incidence onto the Ag{111} surface. The interaction potential of the system is assumed to be pairwise additive. The force between the impinging particle and the surface atom is determined by the Moliere approximation to the Thomas-Fermi potential, with the screening radius being adjusted according to a formula suggested by O'Connor and McDonald.[15] The development of the collision cascade in the Ag substrate is governed by the Morse potential.[16] Our test of the effect of the interaction potential on the sputtering process of Ag atoms from the surface show that the major collision mechanisms that contribute to the sputter intensity do not change significantly as the potential parameters are varied. In addition, a microcrystallite array of atoms with about 350 atoms per layer is utilized to represent the substrate. These atoms are located at the lattice sites corresponding to those for the bulk Ag. As shown in Fig. 1, the azimuthal orientation ϕ of our model system is defined with the right horizontal direction corresponding to the azimuth of $\phi=0°$. The nearest second-layer atoms of the target atom in the first layer of the crystallite are located along the azimuths of $\phi=30°$, 150°, and 270° (the $\langle 2\bar{1}\,\bar{1}\rangle$ directions). The nearest third-layer atoms of the target atom in the first layer are positioned along the azimuths of $\phi=-30°$, 90°, and 210° (the $\langle\bar{2}11\rangle$ directions). These two different ⟨211⟩ directions are along the open spacings between the first-layer atoms.

To obtain statistically reliable results on the angular distribution of the particles sputtered from the surface requires calculations with a large number of incident trajectories. In our calculations, 1840 Ar incident particles are allowed to impinge on the surface and the impacts are uniformly distributed within a symmetry zone located near the center of the microcrystallite that represents the entire surface. Calculations with this large number of impacts are necessary since they allow us to examine, with some degree of statistical reliability, the sputtering dynamics in different regimes of the ejection energy. After

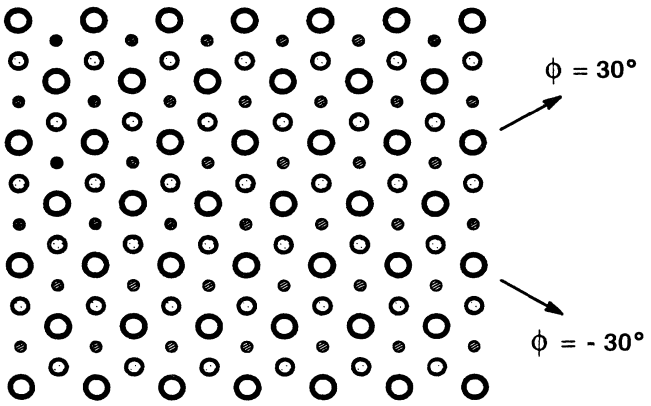

FIG. 1. A portion of the Ag{111} crystal face. The open circles represent the atoms in the first layer, the dotted circles those in the second layer, and the hatched circles those in the third. The orientation of the azimuthal angle (ϕ) is defined from the right horizontal direction.

the primary impact by the incident particle, the trajectories of all the moving atoms in our model system are followed until either their kinetic energies fall below a cutoff value of 0.2 eV or they cross the boundary planes of the microcrystallite. The final position and momentum of the surface atom are used to determine if the atom is ejected, and to calculate its energy and direction of ejection.

III. RESULTS AND DISCUSSION

Presented in Fig. 2 are the angular distributions of Ag atoms that eject from the Ag {111} surface with kinetic energies of some selected values. The distributions are

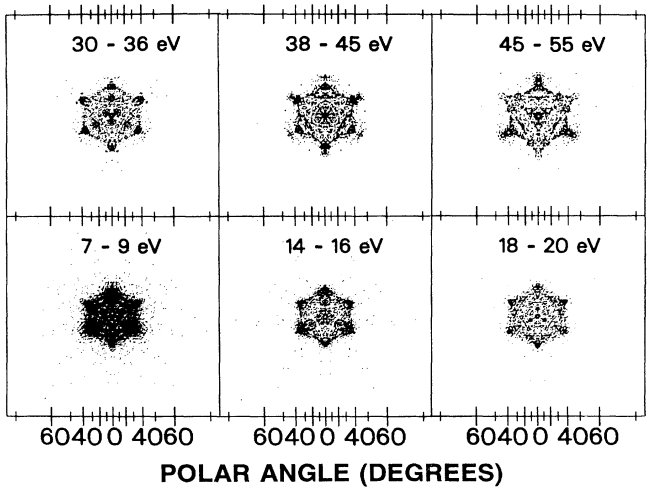

FIG. 2. Spot patterns of ejected Ag atoms from Ag{111}. Each spot represents an ejected atom. The kinetic energy of ejection at which the sputtered atoms are detected is specified at the top of each pattern. The orientation of the pattern is the same as that in Fig. 1.

depicted by the density of spots at which the ejecting Ag atoms intercept an imaginary flat-plate detector located above the sample surface. The angle from the right horizontal direction in the plane of the flat-plate detector corresponds to the azimuthal angle of ejection. The radial distance represents the polar deflection of ejecting particles. As already found both experimentally and theoretically,[9,17] strong azimuthal anisotropies of the threefold symmetry are observed in Fig. 2 at all ejection energies for bombardment on the {111} surface. High densities of spots are found to occur along the open crystallographic directions in the top surface layer where the ejection path is expected to be least obstructed. These directions are along the azimuths of $\langle 2\bar{1}\,\bar{1}\rangle$ and $\langle \bar{2}11\rangle$ for sputtering from the surface of Ag{111}. The reasons that the sputter intensities are higher for ejection along the directions of the open spacings between the first-layer atoms have been discussed before, and were based on the focusing of the moving atoms by the surface atoms along these directions.[17]

Although the high intensities of sputtering in all angular distributions of different ejection energies are always observed along the directions of the open spacings in the top surface layer, significant differences in the sputter intensity are found for ejection along two different $\langle 211\rangle$ azimuths. The intensity at $\langle \bar{2}11\rangle$ is related to the ejection of atoms in the direction of the close-packed row of atoms extending to the bulk along the $\langle 211\rangle$ azimuth, whereas the intensity at $\langle 2\bar{1}\,\bar{1}\rangle$ is related to that in the direction of the non-close-packed row of atoms. We find that at low ejection energies of less than about 15 eV the sputter intensity at $\langle \bar{2}11\rangle$ is always higher than the one at $\langle 2\bar{1}\,\bar{1}\rangle$. It is believed that the higher intensity at $\langle \bar{2}11\rangle$ is associated with the original lattice position of the moving second-layer atom in the crystal with respect to that of the ejected first-layer atom.[17] When a second-layer atom moves up toward the first layer, it has a better chance to collide with a nearest first-layer atom to result in ejection of this first-layer atom along a $\langle \bar{2}11\rangle$ direction than to collide with a second-nearest first-layer atom to cause ejection along $\langle 2\bar{1}\,\bar{1}\rangle$.

It is striking, however, that in the high ejection energy regime the angular distribution is quite dependent upon the ejection energy. The relative sputter intensity between $\langle 2\bar{1}\,\bar{1}\rangle$ and $\langle \bar{2}11\rangle$ azimuths varies as the ejection energy is increased. Presented in Fig. 3(a) is a direct comparison of the $\langle 2\bar{1}\,\bar{1}\rangle$ and $\langle \bar{2}11\rangle$ sputter intensities obtained at a polar angle of 45°. As shown in the figure, the intensity at $\langle \bar{2}11\rangle$ (solid curve) is not always higher than the one at $\langle 2\bar{1}\,\bar{1}\rangle$ (dashed curve) for ejection with kinetic energies of higher than 15 eV. In fact, the two intensities are about the same in the ejection energy regime of between 15 and 45 eV, except at ~20 eV, where the $\langle 2\bar{1}\,\bar{1}\rangle$ intensity is slightly higher than the $\langle \bar{2}11\rangle$ intensity and at ~30 eV, where the intensity at $\langle \bar{2}11\rangle$ is higher. Similar variations with the ejection energy of the relative sputter intensity between $\langle 2\bar{1}\,\bar{1}\rangle$ and $\langle \bar{2}11\rangle$ azimuths can also be observed to a certain extent in the global angular distributions shown in Fig. 2.

Variations in the relative sputter intensity between $\langle 2\bar{1}\,\bar{1}\rangle$ and $\langle \bar{2}11\rangle$ azimuths are much larger at very high

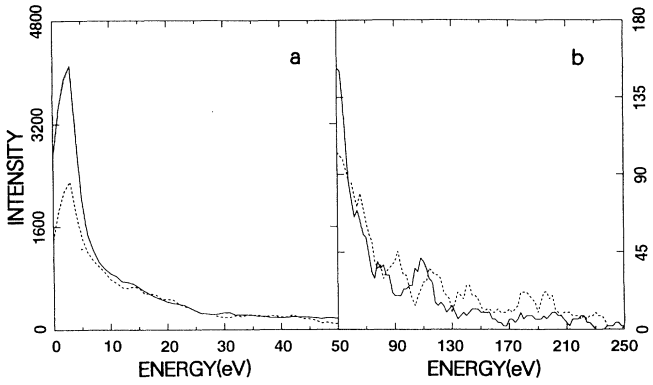

FIG. 3. Calculated ejection energy distributions of Ag atoms emitted from Ag{111} at a polar angle of 45°±10° along $\phi=30°$ (dashed curve) and $\phi=-30°$ (solid curve). The intensity is in the unit of the number of atoms. The bandwidth of the pass energy is assumed in the calculation to be ±2.5 eV for atoms with kinetic energies of less than 50 eV and ±5.0 eV for those with energies of more than 50 eV.

ejection energies. Figure 3(b) shows the sputter intensities at these two azimuths between 50 and 250 eV. As shown in the figure, the intensities along these two $\langle 211\rangle$ crystallographic directions vary relative to each other in an irregular fashion as the kinetic energy of ejection is increased. At ejection energies of between 48 and 55 eV, the sputter intensity is significantly higher at $\langle \bar{2}11\rangle$ than at $\langle 2\bar{1}\,\bar{1}\rangle$. The intensities along these two azimuths become about equal at ejection energies of between 55 and 85 eV. Further increase of the ejection energy to between 85 and 95 eV results in the occurrence of the maximum intensity of ejection along the $\langle 2\bar{1}\,\bar{1}\rangle$ azimuth. As the ejection energy is increased to between 102 and 112 eV, the relative intensity reverses and the intensity along $\langle \bar{2}11\rangle$ becomes higher than the one along $\langle 2\bar{1}\,\bar{1}\rangle$. The azimuthal direction of the maximum intensity alternates again, with the intensity at $\langle 2\bar{1}\,\bar{1}\rangle$ being higher than that at $\langle \bar{2}11\rangle$ for ejection with kinetic energies of more than 120 eV. The observed changes in the relative sputter intensity along different $\langle 211\rangle$ azimuths indicate that there are distinct sputter mechanisms associated with each individual impact that causes surface atoms to eject.[18]

As discussed before, the intensity along $\langle \bar{2}11\rangle$ azimuths is expected to be higher than that along $\langle 2\bar{1}\,\bar{1}\rangle$ because of the arrangement of atoms in the substrate.[17] The higher intensity observed in this study along $\langle 2\bar{1}\,\bar{1}\rangle$ at some selected ejection energies is quite interesting. The sputter mechanisms which result in high intensity along the $\langle 2\bar{1}\,\bar{1}\rangle$ azimuth are thus investigated. In the previous studies,[14,19–22] these mechanisms were usually obtained by numerically following the movement of specific substrate atoms of interest or by analyzing a sequence of snapshots of the bombarded surface. Here, we introduce a time-exposure representation of the collision cascade in the surface. In this representation, the three-dimensional atomic motion in the substrate as well as the atomic movement in the collision-time scale are integrally depicted schematically. It provides a full perception of

the complex *tout ensemble* of energetic particle bombardment on the surface. Shown in Figs. 4, 5, and 6 are the time-exposure representations of the collision cascades in the Ag{111} surface which are induced by bombardment of individual 2-keV Ar particles of normal incidence at specific impact points. The trajectory of each surface atom is portrayed by a string of circles and the time interval between two successive circles is arbitrarily chosen to be ten calculation time steps. The open circle represents the first-layer atom and the size of the circle depicts the vertical displacement of the atom in the substrate. The smaller the circle is, the deeper the atom is displaced into the bulk. In addition, the heaviness of the circle is used to indicate the sequence of the atomic movement in time, with the lighter ones representing the atom in the earlier time steps of the collision cascade. Those atoms which acquire sufficiently large kinetic energies to overcome the surface binding energy and eject into the vacuum are labeled with their final kinetic energies. Finally, the trajectory of the primary particle is marked by a series of symbols, with the plus (+) representing the particle movement above the surface, the cross (×) the movement between the first and the second substrate layers, the upright triangle (△) the movement between the second and the third layers, the inverted triangle (▽) the movement between the third and the fourth layers, and the square (□) the movement underneath the fourth layer. The size of the symbol also depicts the vertical height of the primary particle within the designated space in the substrate.

Studies using this integrated schematic representation of the surface collision cascade show that there are several important collision mechanisms which may result in ejection of the surface atoms along $\langle 2\bar{1}\,\bar{1}\rangle$ azimuths. One mechanism involves the emission of a first-layer atom which is pushed up above the surface by a neighboring first-layer atom moving along a $\langle 2\bar{1}\,\bar{1}\rangle$ direction. As shown in Fig. 4, the primary particle strikes the target atom in the surface and then moves down into the bulk of the crystal. The target atom is thus driven to move along a $\langle 2\bar{1}\,\bar{1}\rangle$ direction, with $\phi \sim 150°$, and into the space between the first and the second layers of the crystal. It in turn forces one of its second-nearest neighbors in the first

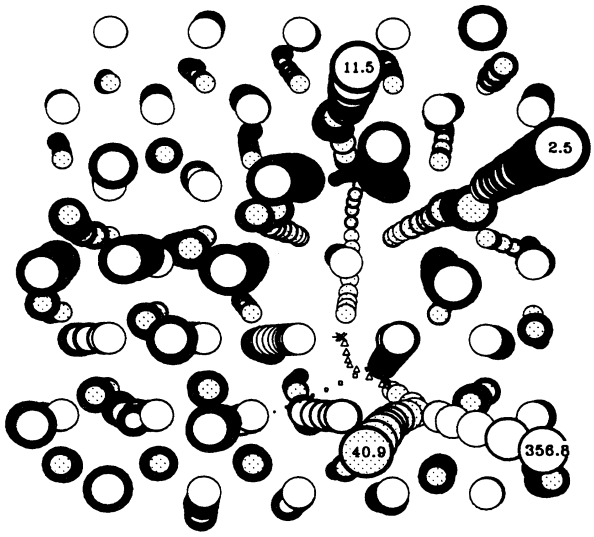

FIG. 5. Time-exposure representation of the energetic particle-induced atomic-collision sequence in the surface. Only the atomic displacement close to the point of the primary impact in the top two atomic layers of the surface is shown.

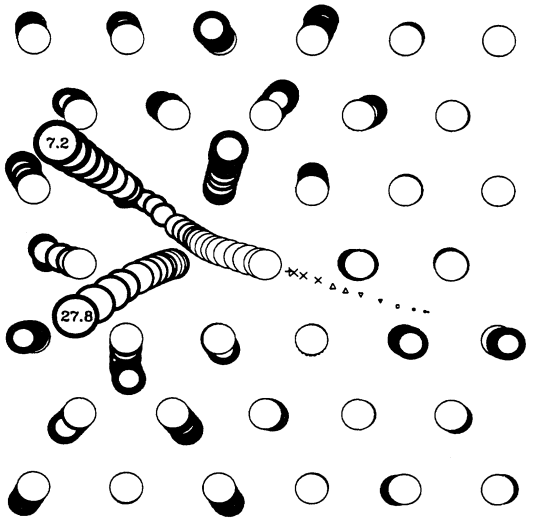

FIG. 4. Time-exposure representation of the energetic particle-induced atomic-collision sequence in the surface. Only the atomic displacement close to the point of the primary impact in the first layer of the surface is shown.

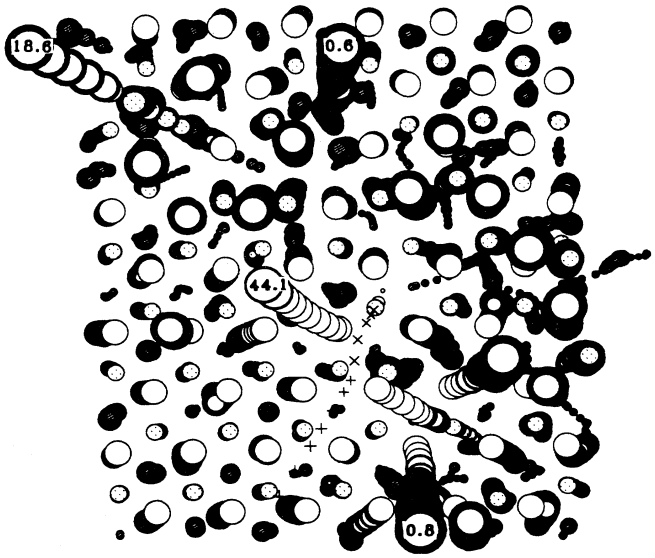

FIG. 6. Time-exposure representation of the energetic particle-induced atomic-collision sequence in the surface. Only the atomic displacement close to the point of the primary impact in the top three atomic layers of the surface is shown.

layer to move upward and to eject from the surface with a kinetic energy of 7.2 eV along the azimuth of $\phi \sim 150°$. This type of the ejection process bears some resemblance to the up-down-collision mechanism reported previously by Harrison and Delaplain for momentum being transmitted through the close-packed string of atoms in the first layer.[23] In our case, the momentum is transmitted through the non-close-packed string of atoms in the first layer along the $\langle 211 \rangle$ azimuth. Further studies show that the up-down-collision sequence may travel quite a distance along $\langle 2\bar{1}\,\bar{1} \rangle$ directions and cause ejection of the surface atoms which are originally located at more than 20 Å away from the point of the primary impact.

The second scattering mechanism which results in atomic emission along $\langle 2\bar{1}\,\bar{1} \rangle$ directions is associated with the alignment of the atomic motion in these directions of ejection. This mechanism is illustrated in Fig. 5, in which the second-layer atoms are represented by dotted circles. As shown in the figure, the 2.5-eV atom ejects from the surface along the azimuth of $\phi \sim 30°$ because of a head-on collision by one of its second-nearest neighbors in the second layer. This second-layer neighboring atom is originally pushed up by one of its own neighbors in the same layer, which in turn is originally knocked downward by the primary particle to move into the space between the second and the third layers of the crystal. This ejection process is somewhat similar to the focuson-type collision mechanism,[24] although in our case the ejection occurs along the direction of the non-close-packed row of atoms which extends from the bulk with a polar angle of 54.7°. Our studies of the successive head-on collisions for atomic emission along $\langle 2\bar{1}\,\bar{1} \rangle$ directions show that this collision sequence may be initiated from as deep as the third atomic layer.

The most important collision mechanism which causes atoms to eject along $\langle 2\bar{1}\,\bar{1} \rangle$ azimuths is, however, associated with the sideswipe of the surface atom by a moving atom in the crystal. With this mechanism, the ejection of a first-layer atom is usually induced by collision of one of its nearest neighbors in the same layer or one of its nearest or third-nearest neighbors in the second layer. For example, the 0.8-eV atom in Fig. 6 is forced to move upward along the azimuth of $\phi \sim 270°$ by a skip hit of its nearest neighbor in the first layer. This first-layer neighbor is originally knocked away from its lattice position by the primary particle to travel along the azimuth of $\phi \sim 330°$. The sideswipe collision process usually results in ejection of atoms with low kinetic energies.

Ejection along $\langle 2\bar{1}\,\bar{1} \rangle$ azimuths may also be caused directly by the collision of the primary particle. In this case, atoms may be pushed out of the surface by the primary particle which is either moving down into the crystal, traveling within the space between surface layers, or returning from the bulk. The mechanistic details of the ejection process due to the collision by the primary particle are similar to that of the three processes (the up-down-, the head-on-, and the sideswipe-collision sequences) discussed above. For example, as shown in Fig. 6, the incident particle drives a second-layer atom down into the bulk upon the primary impact on the surface. It then moves into the space between the first and the second layers of the crystal. When traveling in this space, it sideswipes an atom in the first layer and causes it to take off with a kinetic energy of 44.1 eV along the azimuth of $\phi \sim 150°$. The primary particle then emerges from the surface at a distance of about 2.9 Å away from the point of the primary impact. We note that Fig. 6 also shows the ejection of a first-layer atom which takes off with a kinetic energy of 18.6 eV along the azimuth of $\phi \sim 150°$. This ejection is due to a sequence of successive head-on collisions which is initiated from the third surface layer. (The third-layer atoms are represented in Fig. 6 by hatched circles).

Variations with the ejection energy of the angular distribution of sputtered atoms may pose some limitations in the experimental determination of surface structures using angle-resolved mass spectrometry. As we have discussed before, the existing ejection theory[5,8] predicts that the desorption of particles from the surface due to the energetic incident collision is strongly influenced by the presence of the open spacings between the first-layer atoms and by the atomic arrangement in the crystal. Thus, the angular distribution of ejected particles should reflect the geometric structure of the surface if the high-energy particles are detected. Results from our present study, however, indicate that this simple approach to determine the structure of solid surfaces may be applied only if the ejection energy dependence of the angular distribution is also known.

It is theoretically interesting to see if other detection parameters exist which may provide angular distributions with little variations in the relative sputter intensity between $\langle 2\bar{1}\,\bar{1} \rangle$ and $\langle \bar{2}11 \rangle$ directions. Results of our studies show that the selection for detection of the ejected atoms based on the collision time, instead of the ejection

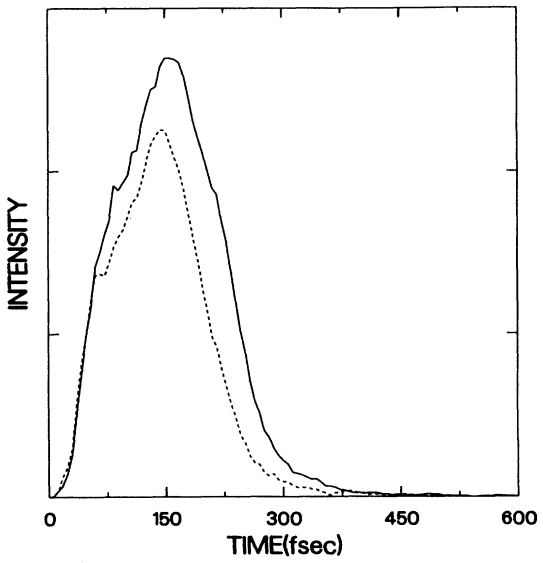

FIG. 7. Calculated collision-time distributions of Ag atoms ejected from Ag{111} at a polar angle of 45°±10° along $\phi = 30°$ (dashed curve) and $\phi = -30°$ (solid curve).

energy, may be utilized for obtaining angular distributions with fewer alternations in the maximum sputter intensity between these two directions. Here, the collision time is defined as the time interval between the instant of the primary impact on the surface and the moment when an emitting surface atom passes the cutoff boundary of the interaction potential, which in this study is chosen to be at a distance of 5 Å from the surface. In Fig. 7, the dependences on the collision time of the sputter intensities along $\langle 2\bar{1}\,\bar{1}\rangle$ and $\langle \bar{2}11\rangle$ directions are shown. On the whole, the intensity along the $\langle \bar{2}11\rangle$ direction (solid curve) is greater than the one along the $\langle 2\bar{1}\,\bar{1}\rangle$ direction (dashed curve), although the relative intensity between the two directions changes as the "collision-time window" is tuned for ejected atoms. In particular, at the collision time of above ~ 50 fsec the sputter intensity along $\langle \bar{2}11\rangle$ is almost always higher than the one along $\langle 2\bar{1}\,\bar{1}\rangle$. It suggests that the collection of the sputtered atoms of all energies and long collision times may be applied for providing significant information about the geometric structure of the surface.

IV. CONCLUSIONS

The angular distributions of ejected atoms from a Ag{111} surface are calculated from classical dynamics simulations of the particle surface collision process. At low ejection energies, the distributions are well predicted by the existing ejection theory. However, as the kinetic energy of ejection is increased to about 15 eV, the preferred direction of ejection alternates between two different $\langle 211\rangle$ azimuths. To explore the genetics of the ejection process which results in atoms taking off from the surface along particular crystallographic directions, an integrated schematic representation of the collision cascade is introduced. In this representation, the three-dimensional atomic displacement sequences in the surface are depicted in a collision-time scale. It shows that the peak azimuth of ejection may be decided by the presence of the open spacing in the top surface layer, the atomic arrangement in the crystal, and the details of the atomic collision process in the substrate. Collision mechanisms such as the up-down, the head-on, and the sideswipe processes may all contribute to the sputter intensity obtained along the non-close-packed $\langle 211\rangle$ direction. In particular, the sideswipe-collision mechanism, in which the surface atom is ejected due to a skip hit by a moving particle in the crystal, contributes most to the sputter intensity. Except being hit by the energetic primary particle, atoms desorbed through this mechanism generally have low kinetic energies of ejection.

The alternation of the maximum intensity of sputtering in the angular distribution of ejected atoms may pose some difficulties in the experimental determination of the surface structure using angle-resolved mass spectrometry. However, with the aid of the computer simulation of the collision process in the surface, the dependence of the angular distribution on the ejection energy may be fully utilized to explore some complex surface structures. For example, chemisorption of Ag on Si$\{111\}$[25–28] causes significant structural changes in the Si surface. There has been no consensus as to the exact structure formed at low Ag dosages and to the vertical distance of the Ag atom relative to the Si atomic layer. Depending on the height and the location of Ag relative to that of Si the variation of the Ag and Si angular distributions with the ejection energy is expected to be different for the different structural models proposed.

Studies using our time-exposure schematic representation of the collision cascade also reveals interesting surface phenomena related to the collision of energetic particles on the surface. Although there are incidences which develop collision cascades of considerable complexity,[29] some of them induce very simple collision sequences in the surface. On the whole, this representation shows that under static keV particle bombardment, the crystal structure near the target atom of the surface may not be severely damaged. Confirmation of this observation will, however, require further study.

[1] C. T. Reimann, K. Walzl, M. El-Maazawi, D. M. Deaven, B. J. Garrison, and N. Winograd, J. Chem. Phys. **89**, 2539 (1988).

[2] C.-C. Chang and N. Winograd, Phys. Rev. B **39**, 3467 (1989).

[3] L. L. Lauderback and S. A. Larson, Surf. Sci. **234**, 135 (1990).

[4] F. Masson, H. Bu, M. Shi, and J. W. Rabalais, Surf. Sci. **249**, 313 (1991).

[5] N. Winograd, B. J. Garrison, and D. E. Harrison, Jr., Phys. Rev. Lett. **41**, 1120 (1978).

[6] J. W. Rabalais, CRC Crit. Rev. Solid State Mater. Sci. **14**, 319 (1988).

[7] S. P. Holland, B. J. Garrison, and N. Winograd, Phys. Rev. Lett. **44**, 756 (1980).

[8] N. Winograd, in *Chemistry and Physics of Solid Surfaces V*, edited by R. Vanselow and R. Howe, Springer Series in Chemical Physics Vol. 35 (Springer-Verlag, Berlin, 1983), p. 403.

[9] N. Winograd, P. H. Kobrin, G. A. Schick, J. Singh, J. P. Baxter, and B. J. Garrison, Surf. Sci. **176**, L817 (1986).

[10] C.-C. Chang and N. Winograd, Surf. Sci. **230**, 27 (1990).

[11] L. L. Lauderback, A. J. Lynn, C. J. Waltman, and S. A. Larson, Surf. Sci. **243**, 323 (1991).

[12] R. A. Gibbs, S. P. Holland, K. E. Foley, B. J. Garrison, and N. Winograd, J. Chem. Phys. **76**, 684 (1982).

[13] C.-C. Chang, Mater. Res. Soc. (to be published).

[14] D. E. Harrison, Jr., CRC Crit. Rev. Solid State Mater. Sci. **14**, S1 (1988); N. Winograd, B. J. Garrison, and D. E. Harrison, Jr., J. Chem. Phys. **73**, 3473 (1980).

[15] D. J. O'Connor and R. J. McDonald, Radiat. Eff. **34**, 247 (1977).

[16] C.-C. Chang, SIA Surf. Interface Anal. **15**, 79 (1990).

[17] B. J. Garrison, C. T. Reimann, N. Winograd, and D. E. Harrison, Jr., Phys. Rev. B **36**, 3516 (1987).

[18] B. J. Garrison, N. Winograd, and D. E. Harrison, Jr., Surf. Sci. **87**, 101 (1979).

[19] D. E. Harrison, Jr., Radiat. Eff. **70**, 1 (1983).

[20] R. P. Webb and D. E. Harrison, Jr., Nucl. Instrum. Methods B **2**, 660 (1984); Phys. Rev. Lett. **50**, 1478 (1983); J. Appl. Phys. **53**, 5243 (1982).

[21]B. J. Garrison, N. Winograd, and D. E. Harrison, Jr., Phys. Rev. B **18**, 6000 (1978).
[22]R. Smith, D. E. Harrison, Jr., and B. J. Garrison, Phys. Rev. B **40**, 93 (1989).
[23]D. E. Harrison, Jr. and C. B. Delaplain, J. Appl. Phys. **47**, 2252 (1976).
[24]R. H. Silsbee, J. Appl. Phys. **28**, 1246 (1957).
[25]E. L. Bullock, G. S. Herman, M. Yamada, D. J. Friedman, and C. S. Fadley, Phys. Rev. B **41**, 1703 (1990).
[26]W. C. Fan, A. Ignatiev, H. Huamg, and S. Y. Tong, Phys. Rev. Lett. **62**, 1516 (1989).
[27]T. L. Porter, C. S. Chang, and I. S. T. Tsong, Phys. Rev. Lett. **60**, 1739 (1988).
[28]T. Takahashi, S. Wakatani, N. Okamoto, T. Ishikawa, and S. Kikuta, Jpn. J. Appl. Phys. **27**, L753 (1988).
[29]R. Smith and D. E. Harrison, Jr., Phys. Rev. B **40**, 2090 (1989).